



Enhancement of crystal violet dye adsorption on *Artocarpus camansi* peel through sodium hydroxide treatment

Hei Ing Chieng^a, Linda B.L. Lim^{a,*}, Namal Priyantha^{b,c}

^aDepartment of Chemistry, Faculty of Science, Universiti Brunei Darussalam, Jalan Tungku Link, Gadong, Bandar Seri Begawan, Negara Brunei Darussalam

Tel. 00-673-8748010; email: linda.lim@ubd.edu.bn (L.B.L. Lim), huiing.250@hotmail.com (H.I. Chieng)

^bDepartment of Chemistry, Faculty of Science, University of Peradeniya, Peradeniya, Sri Lanka

^cPostgraduate Institute of Science, University of Peradeniya, Peradeniya, Sri Lanka
Email: namal.priyantha@yahoo.com

Received 22 March 2016; Accepted 1 June 2016

ABSTRACT

This study investigated the potential use of breadnut peel (KS) and NaOH-KS for the removal of crystal violet (CV) dye from aqueous solution. The adsorption capacity of KS was enhanced from 275 mg g⁻¹ to 479 mg g⁻¹ after NaOH treatment. The adsorbents were characterized using FTIR, SEM and XRF. Thermodynamics studies showed that the adsorption process was endothermic and adsorption kinetics for NaOH-KS followed the pseudo second order. Regeneration studies showed that NaOH-KS adsorbed CV even after five consecutive cycles. The NaOH-KS has strong adsorption and regenerating abilities coupled with fast kinetics, and is therefore a promising low-cost adsorbent for CV removal.

Keywords: Breadnut peel; Chemical treatment; Crystal violet dye; Adsorption equilibrium; Kinetics; Regeneration

1. Introduction

Industrialization and urbanization are increasing in response to the needs of the global population of over seven billion. This comes at a price, because more pollutants are being introduced into the environment through industrial emissions. Industrial effluents containing pollutants such as heavy metals and toxic dyes are detrimental to human health if they are not removed. In recent decades, much attention has been focused on cleaning up wastewater. Clean-up methods must be effective, economical, and simple. In this context, attention has recently been turned to the use of adsorption techniques [1–3]. Low-cost adsorbents derived from industrial and agricultural wastes [4–6], and natural substances such as peat [7–10] and plant materials [11–16] have been successfully used to remove various types of pollutants.

Artocarpus fruit wastes (skin and core) generally make up more than 60% of the fruit [17,18]. This study focuses on the use of *A. camansi* (Kemangsi) peel (KS), which has no economic value and is discarded as waste, for the removal of a toxic cationic crystal violet (CV) dye, also known as methyl violet 10B. This dye has been reported to show dose-related carcinogenic potential at different organ sites when tested in mice [19]. CV is poisonous to human mammalian cells and is a strong mutagen. It can cause eye irritation and permanent injury to the cornea and conjunctiva. CV can also irritate the respiratory tract if inhaled, causing vomiting, headache, diarrhea, and dizziness. Long-term contact with CV may cause damage to the gastrointestinal tract [20,21]. *Artocarpus* wastes can be used as low-cost biosorbents for the removal of heavy-metal ions and toxic dyes. For example, cores of *A. camansi* (breadnut) and *A. odoratissimus* (tarap) have been used to remove methylene blue [22] and toxic heavy metals such as Cu(II) and Cd(II) [23,24], while various *Artocarpus* peels, including peels from

* Corresponding author.

its hybrids, have been successfully used for the removal of dyes and heavy metals [13,14,25–27].

The main objectives of this work were to characterize natural and NaOH-treated KS (NaOH-KS), and to compare their CV-adsorption capacities to quantify enhancement of the adsorption properties by chemical treatment. The adsorption kinetics of the treated adsorbent was also investigated to confirm enhancement of the CV-adsorption properties. Regeneration studies were performed to investigate the potential reuse of NaOH-KS after CV adsorption. This is an important consideration in designing economically viable methods for the treatment of CV in real effluents.

2. Experimental

2.1. Materials and sample preparation

A. camansi (Kemangsi) fruits were randomly purchased from the local open market. The KS, which was separated from the rest of the fruit, was oven dried at 60°C until a constant mass was obtained. The dried KS was powdered and sieved; the fraction of particle size 355 to 850 µm was used for the experiments. Chemical treatment was performed by shaking KS (1.00 g) in 4.0 M NaOH (100 mL) overnight. The NaOH-KS was then filtered and washed with double-distilled water to remove excess NaOH. The NaOH-KS was dried in an oven at 60°C until a constant mass was obtained.

CV (molecular formula C₂₅H₃₀N₃Cl, molecular weight 407.98, λ_{max} 589.5 nm) was purchased from Sigma Chemicals, Singapore. All chemicals and reagents were used without prior purification. All experiments were performed in triplicate unless otherwise stated to validate the experimental results. All shaking experiments were performed on an orbital shaker at 250 rpm at ambient temperature unless otherwise stated. The adsorbent:dye solution ratio was kept at 1:500 (weight:volume) throughout the experiments.

2.2. Adsorption studies

The effect of contact time was investigated by mixing KS with 100 mg L⁻¹ CV on an orbital shaker for time intervals of 30 to 240 min. The solution was then filtered through a fine stainless-steel sieve (pore size 355–850 µm) and the CV concentration was determined by measuring the absorbance at 590 nm using an ultraviolet-visible (UV-vis) spectrophotometer (Shimadzu Model UV-1601PC). Subsequent adsorption reactions were performed using the optimum contact time.

The effect of pH was studied by determining the extent of dye removal in solutions of various pHs ranging from 2 to 10. The pH was adjusted by addition of 0.1 M HNO₃ and/or 0.1 M NaOH. The effect of ionic strength on CV removal was studied using solutions of ionic strengths ranging from 0.1 to 1.0 M KNO₃.

Batch adsorption studies were performed using CV of initial concentrations from 0 to 1,000 mg L⁻¹. The amount of CV adsorbed, q_e (mg g⁻¹), and the percentage removal of CV were calculated using Eqs. (1) and (2):

$$q_e = \frac{C_i - C_e}{m} \times V \quad (1)$$

$$\text{Removal (\%)} = \frac{C_i - C_e}{C_i} \times 100 \quad (2)$$

where C_i and C_e are the initial and equilibrium CV concentrations (mg L⁻¹), respectively. V is the volume of solution (L) and m is the mass of the biosorbent (g). Thermodynamic studies were performed using CV concentrations of 0 to 1,000 mg L⁻¹ at selected temperatures ranging from 298 to 343 K in a temperature-controlled shaker bath using the optimum contact time. After treatment at each temperature, the supernatant was filtered and the UV-vis absorbance was recorded to determine the concentration of un-adsorbed CV left in solution. The results were used to determine thermochemical parameters using standard relationships.

2.3. Kinetics studies

The adsorption kinetics of natural and NaOH-KS were studied by agitating 1,000 mg L⁻¹ CV solution at room temperature. Small aliquots of the dye solution were withdrawn at 1-min intervals until equilibrium was reached. The concentration of CV left in solution was determined, and the validities of various kinetic models were tested.

2.4. Regeneration studies

Regeneration studies were performed by loading NaOH-KS and a 100 mg L⁻¹ CV solution in a 1:500 ratio and agitating for 2 h. The CV-loaded NaOH-KS was dried overnight in an oven at 60°C. The CV was desorbed from NaOH-KS by agitating with 250 mL of 0.1 M HNO₃, 0.1 M NaOH, or water for the optimum contact time. A control was kept for the same time period to compare the removal/adsorption capacity with that of the desorbed adsorbent. The desorbed solution and regenerated NaOH-KS were separated and the filtrate was analyzed using UV-vis spectroscopy. The amounts of adsorbed and desorbed CV were determined for at least five consecutive regeneration cycles to estimate the regenerating ability of NaOH-KS.

3. Results and discussion

3.1. Adsorbent characterization

Scanning electron microscopy (SEM) images showed that the porosity of the KS surface increased on treatment with NaOH solution (Fig. 1(a) and (c)). This could be partly caused by alkaline degreasing, which would remove oil or surface impurities from the KS's surface [28]. The adsorption capacity of NaOH-KS was expected to increase with increasing surface porosity. Fig. 1(b) and (d) showed the surfaces of KS and NaOH-KS after dye adsorption. A comparison of Fig. 1(a) and (c) with (b) and (d) showed that treatment with CV resulted in the formation of a layer of CV on the surfaces of KS and NaOH-KS, and filling of the pores and cavities can be observed.

Functional group characterization of NaOH-KS, using Fourier-transform infrared (FTIR) spectroscopy showed that the broad –OH band at 3,420 cm⁻¹ shifted to 3,402 cm⁻¹ after CV adsorption. The band at 1,622 cm⁻¹ became sharper and shifted to 1,589 cm⁻¹, indicating interactions of –COO and N–H groups of CV on the surface of NaOH-KS. The adsorption

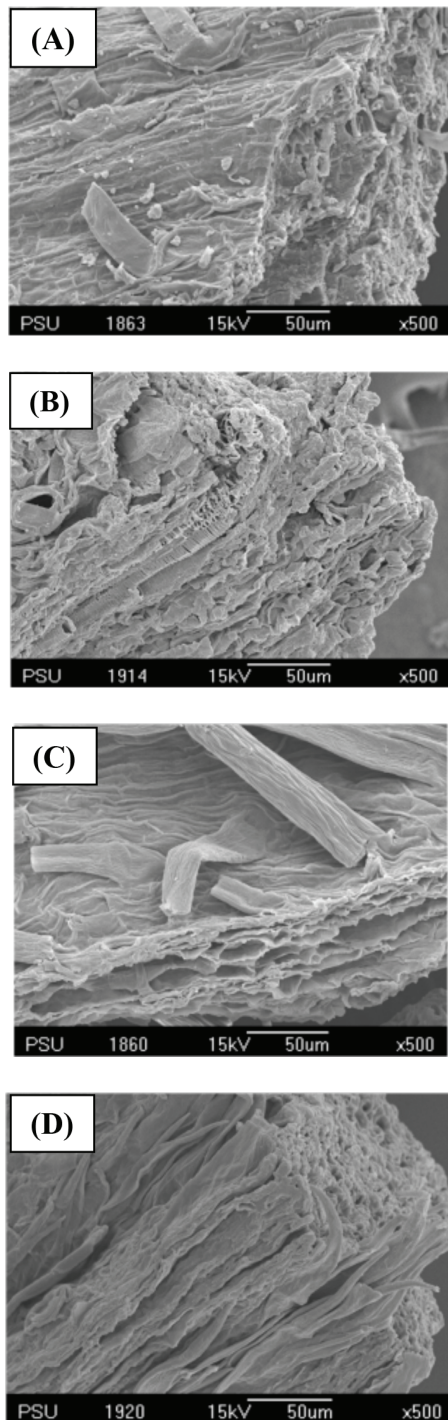


Fig. 1. SEM images showing surface morphologies of (a) KS, (b) KS-CV, (c) NaOH-KS, and (d) NaOH-KS-CV at 500 \times magnification.

bands at 1,426 and 1,332 cm^{-1} were replaced by a new band at 1,364 cm^{-1} , which is attributed to symmetric stretching of the $-\text{COO}$ group. Two new bands observed at 1,298 and 1,175 cm^{-1} after CV adsorption may be related to C–O stretching and C–N or sulfonic groups [29]. The bands at 956 and 895 cm^{-1} , which shifted to 941 and 829 cm^{-1} , respectively, may arise from aromatic C–H bending on the NaOH-KS's surface.

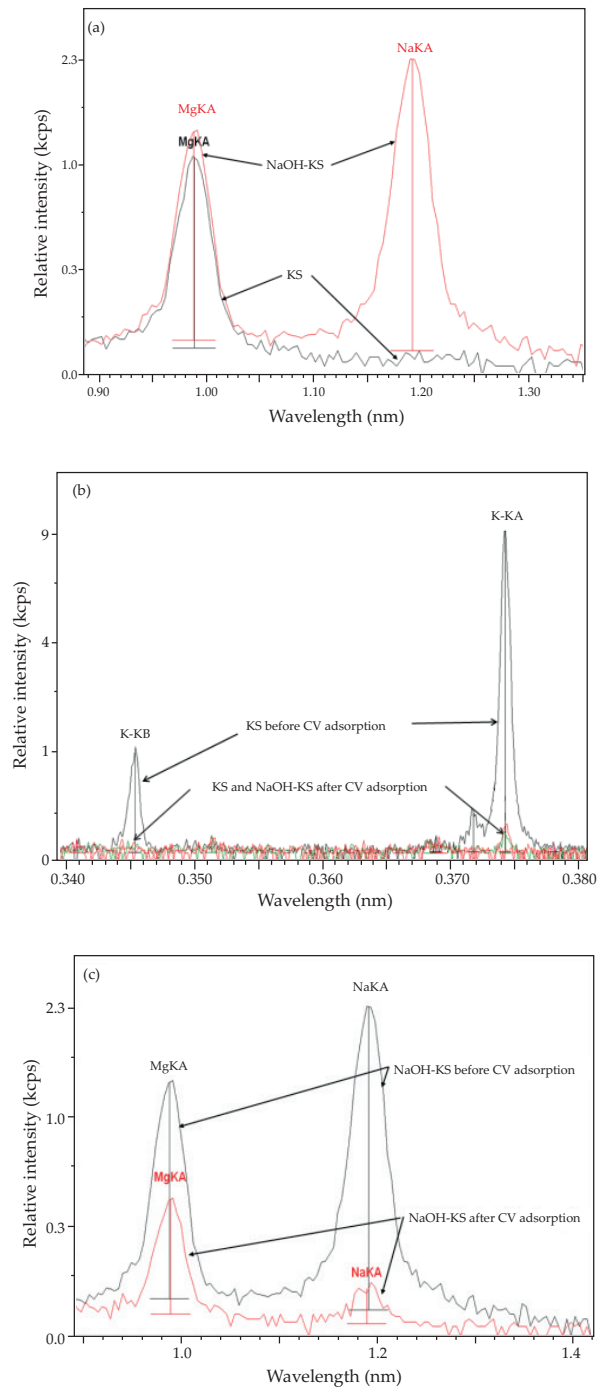


Fig. 2. XRF spectra of (a) KS and NaOH-KS (Na peak), (b) K peak before and after CV adsorption, and (c) Na peak before and after CV adsorption.

Elemental analyses of the KS and NaOH-KS surfaces, before and after CV adsorption, were performed using X-ray fluorescence (XRF) spectroscopy. The results showed that on treatment with base, the amount of Na which was initially undetected in KS increased to approximately 19% in NaOH-KS (Fig. 2(a)). This shows that acidic functional moieties, mainly phenolic and carboxylic groups of KS,

react with NaOH to form Na salts, as shown in Reaction (1) below:



The anionic forms of these functional groups would readily attract cationic CV species, releasing Na^+ back into the solution. This explains the significant decrease in the Na content of NaOH-KS after CV treatment, as shown in Fig. 2(c).

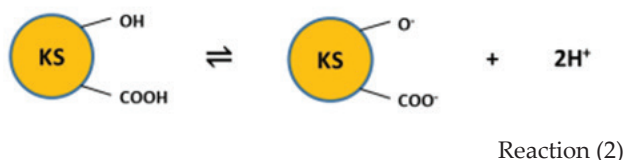
The XRF spectra in Fig. 2(b) showed that the adsorption of CV on KS decreased the amount of K to about 0.2%. This could be because cationic CV replaces K^+ on the adsorbent's surface. Similar observations have previously been reported for the removal of methylene blue [14], methyl violet 2B [30], and rhodamine B [31]. The decrease in the Mg content after treatment with CV provides further support for the above argument (Fig. 2(c)).

3.2. Effect of contact time

KS removed >50% CV within the first 15 min. CV adsorption onto NaOH-KS was more rapid and reached adsorption equilibrium faster; a larger percentage of CV, i.e., 70%, was removed within a shorter time period, i.e., 5 min (Fig. 3). Careful consideration of the changes in the extent of removal as a function of time showed that the optimum contact time for CV adsorption by both KS and NaOH-KS was 120 min.

3.3. Effect of pH

The solution pH is an important parameter in adsorption studies because it controls the process chemistry. A change in the pH can change the surface properties of adsorbents and cause adsorbate molecules to ionize or dissociate. As can be seen from Fig. 4, both KS and NaOH-KS were ineffective in removing CV in a strongly acidic medium (pH 2). In such a medium, all the acidic functionalities are in neutral forms and the following equilibrium shifts to the left on addition of excess H^+ ions (Reaction 2).



These conditions are therefore not conducive to interactions of CV species. However, both KS and NaOH-KS effectively removed CV at the natural pH, 4.71, at percentages comparable with or better than those at other pHs in the range of 3 to 10. However, a higher pH promotes Reaction (1), increasing the negative charge density of the adsorbent and thereby increasing the adsorption ability of cationic CV. Good removal of CV was obtained at its natural pH; therefore, no pH adjustment was needed, and the natural pH

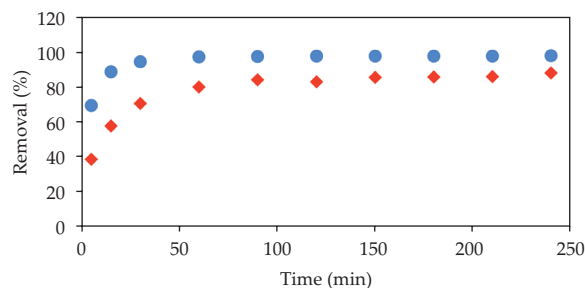


Fig. 3. Effect of contact time on adsorption of CV on KS (♦) and NaOH-KS (●) (0.050 g adsorbent, 25.0 mL of 100 mg L⁻¹ CV, 250 rpm shaking).

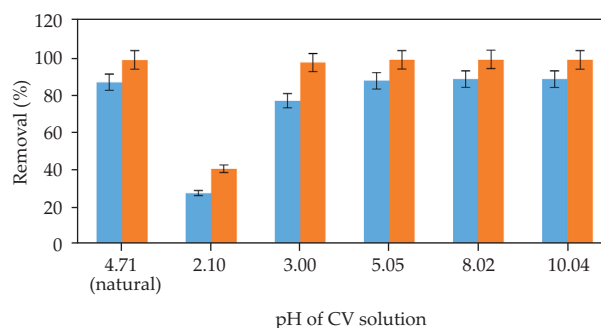


Fig. 4. Effect of pH on adsorption of CV by KS (●) and NaOH-KS (●) (0.050 g adsorbent, 25.0 mL of 100 mg L⁻¹ CV, 250 rpm shaking).

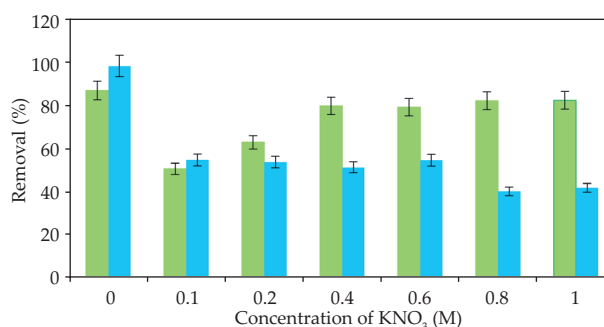


Fig. 5. Effect of ionic strength on CV adsorption by KS (●) and NaOH-KS (●) (0.050 g adsorbent, 25.0 mL of 100 mg L⁻¹ CV, 250 rpm shaking).

was used throughout the study. These conditions make this method a potential low-cost, fast wastewater treatment.

3.4. Effect of ionic strength

Wastewater often contains salts; these may lead to high ionic strengths, resulting in decreased adsorption efficiency. It is therefore important to investigate the dependence on ionic concentration of metal ion removal. The adsorptions of CV by KS and NaOH-KS both depend on the concentration of KNO_3 , as shown in Fig. 5. The CV-adsorption abilities of both

adsorbents decreased by about 40% in 0.1 M KNO_3 . Similar observations have previously been reported for the adsorption of cationic dyes by various adsorbents such as duckweed [32] and peat [33]. A comparison of the performances of KS and NaOH-KS showed that the former has a better overall resilience to the effect of ionic strength. NaOH-KS was ineffective in CV removal at all KNO_3 concentrations from 0.1 to 1 M. This shows that although NaOH-KS is much better than KS for the removal of CV dye, the ionic environment interferes less in the case of untreated KS.

3.5. Adsorption isotherms and error functions

Equilibrium adsorption isotherms provide useful information on the interactions between adsorbents and adsorbates [34]. The adsorption isotherms of CV onto both KS and NaOH-KS, obtained through batch experiments, indicated that NaOH treatment significantly enhances the adsorption ability of the adsorbent (Fig. 6(a)). Saturation of the NaOH-KS's surface takes a shorter time because of the negatively charged surface moieties. The adsorption data obtained were fitted to the linear and non-linear isotherm models listed in Table 1, and analyzed based on six error functions, i.e., average relative error (ARE), sum of square errors (SSE), the Hybrid fractional error function (HYBRID), sum of absolute errors (EABS), the Marquardt's percentage standard deviation (MPSD) and non-linear chi-squared test (χ^2). The non-linear isotherm plot for each isotherm model is shown in Fig. 6(b) and (c) and the adsorption parameters determined from each isotherm are given in Table 1. The suitability of the isotherm models for describing CV adsorption onto KS or NaOH-KS was determined by comparison of the correlation coefficient (R^2) values, simulation of non-linear isotherms, and from the error values (Table 2).

Because of the uncertainties and limitations of R^2 values, the error functions shown in Table 2 provided better accuracies for selecting the most suitable isotherm models. The $q_{e,\text{calc}}$ (calculated) and $q_{e,\text{meas}}$ (measured) values in the error functions are the calculated and measured adsorption capacities, respectively; n represents the number of data points, and p denotes the number of parameters.

Of the six different isotherm models used in this study, the Dubinin–Radushkevich (D–R) model [35], which is used to estimate the porosity and apparent free energy, gave the highest overall error values for both KS and NaOH-KS. This is confirmed by Fig. 6(b) and (c), which showed a large deviation from the experimental isotherm. The Temkin model [36] provides information on the heat of adsorption, which decreases linearly with increasing surface coverage, because of the uniform distribution of the binding energies. Although the Temkin isotherm model gave a good R^2 of approximately 0.95 for both the adsorbents, its overall error values were high, and it was therefore deemed to be unsuitable. The worst linear regression for NaOH-KS was that for the Redlich–Peterson (R–P) isotherm model, with $R^2 = 0.4903$ (not shown in Fig. 8).

The Freundlich isotherm model [37] is an empirical equation based on multilayer adsorption; it assumes that the adsorption energy decreases exponentially during the equilibrium stage. According to the linear regression, error values, and non-linear isotherm plots, the Freundlich isotherm

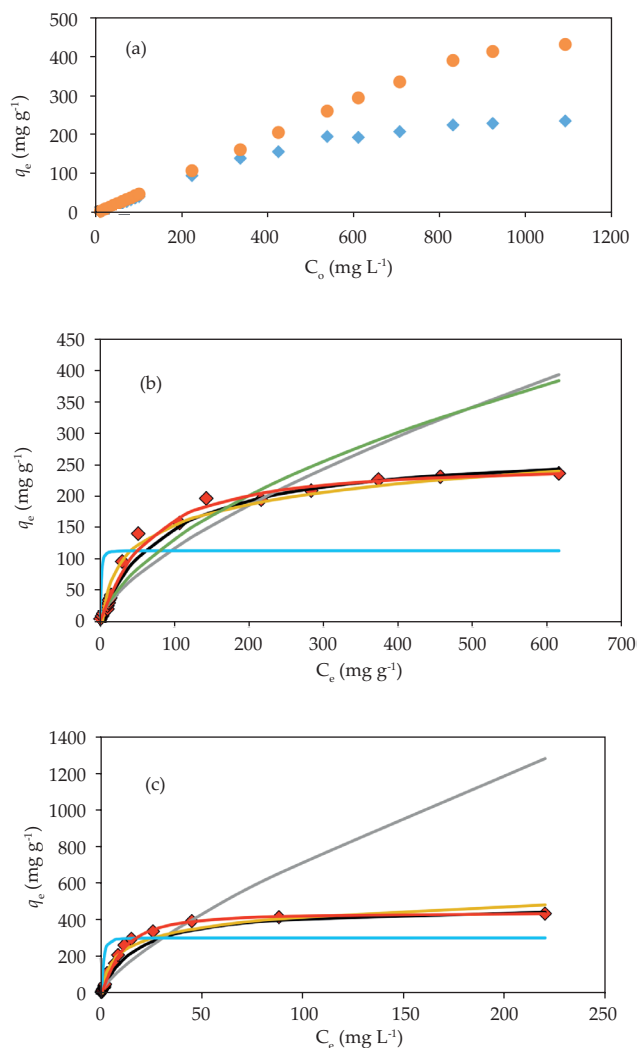


Fig. 6. Isotherms for CV adsorption (a) on KS (\blacklozenge) and NaOH-KS (\bullet), experimental isotherms and simulated isotherm models for adsorption of CV on (b) KS and (c) NaOH-KS [(\blacklozenge) experimental data; (\blacksquare) Langmuir; (\blacktriangle) Freundlich; (\blacklozenge) Temkin; (\bullet) D-R; (\blacktriangle) R-P; (\blacktriangle) Sips].

model is not suitable for describing the adsorption of CV onto KS and NaOH-KS. Of the six isotherm models used, the Langmuir model [38] and the Sips model [39] are comparable, with high linear regressions close to unity, and with the lowest overall errors. In contrast, CV adsorption by NaOH-KS is better fitted to the Sips model, which gave a higher R^2 with lower overall errors.

The Langmuir isotherm assumes that the maximum adsorption corresponds to saturated monolayer adsorption on a homogeneous adsorbent surface and that no further adsorption can take place after equilibrium has been reached. This model also signifies that adsorption is monolayer and that there are no interactions between adsorbed molecules at neighboring sites. The Sips isotherm is a three-parameter isotherm model, and is a combination of the Langmuir and Freundlich isotherms. At low adsorbate concentrations, this isotherm reduces to the Freundlich form; at high adsorbate

Table 1
Various isotherm models and parameters for adsorption of CV on KS and NaOH-KS at 298 K

Isotherm model	Non-linear	Linear	Parameter	KS	NaOH-KS
Langmuir	Non-linear	$q_e = \frac{K_L q_{max} C_e}{1 + K_L C_e}$	K_L (L mg ⁻¹)	0.011	0.056
	Linear	$\frac{C_e}{q_e} = \frac{1}{K_L q_{max}} + \frac{C_e}{q_{max}}$	q_{max} (mg g ⁻¹)	275.00	479.00
	Plot	$\frac{C_e}{q_e}$ vs C_e	R^2	0.9895	0.9817
Freundlich	Non-linear	$q_e = K_F C_e^{1/n}$	K_F (mg g ⁻¹)	5.31	24.14
	Linear	$\ln q_e = \frac{1}{n} \ln C_e + \ln K_F$	$1/n$	0.67	0.74
	Plot	$\ln q_e$ vs $\ln C_e$	R^2	0.9398	0.8831
Temkin	Non-linear	$q_e = \frac{RT}{b_T} \ln K_T C_e$	K_T (L mg ⁻¹)	0.25	1.37
	Linear	$q_e = \frac{RT}{b_T} \ln K_T + \frac{RT}{b_T} \ln C_e$	b_T (J mol ⁻¹)	52.12	29.42
	Plot	q_e vs $\ln C_e$	R^2	0.9447	0.9517
Dubinin–Radushkevich (D–R)	Non-linear	$q_e q_{max} \exp(-\beta \varepsilon^2)$ $\varepsilon = RT \ln \left[1 + \frac{1}{C_e} \right]$ $E = \frac{1}{\sqrt{2\beta}}$	q_{max} (mg g ⁻¹)	112.81	300.67
	Linear	$\ln q_e = \ln q_{max} - \beta \varepsilon^2$	E (J mol ⁻¹)	886	1310
	Plot	$\ln q_e$ vs ε^2	R^2	0.7041	0.9401
Redlich–Peterson (R–P)	Non-linear	$q_e = \frac{K_R C_e}{1 + a_R C_e^\alpha}$	K_R (mg g ⁻¹)	4.40	400.00
	Linear	$\ln \left(K_R \frac{C_e}{q_e} - 1 \right) = \alpha \ln C_e + \ln a_R$ where $0 \leq \alpha \leq 1$	a_R (L mg ⁻¹)	0.22	15.63
	Plot	$\ln \left(K_R \frac{C_e}{q_e} - 1 \right)$ vs $\ln C_e$	α	0.52	0.27
Sips	Non-linear	$q_e = \frac{q_{max} K_S C_e^{1/n}}{1 + K_S C_e^{1/n}}$	q_{max} (mg g ⁻¹)	0.8064	0.4903
	Linear	$\ln \left(\frac{q_e}{q_{max} - q_e} \right) = \frac{1}{n} \ln C_e + \ln K_S$	K_S (L mg ⁻¹)	252.00	440.00
	Plot	$\ln \left(\frac{q_e}{q_{max} - q_e} \right)$ vs $\ln C_e$	$1/n$	0.0091	0.050
			R^2	1.14	1.31
			R^2	0.9897	0.9964

q_e is the amount of dye adsorbed, C_e is the equilibrium concentration of the dye, q_{max} is the maximum adsorption capacity (mg g⁻¹), K_L (L mg⁻¹) and K_F (mg^{1-1/n} L^{1/n} g⁻¹) are the Langmuir and Freundlich constants, respectively, n is an empirical parameter related to adsorption intensity, K_T is the equilibrium binding constant (L mg⁻¹) corresponding to the maximum binding energy, constant B is related to the heat of adsorption, R is the gas constant, T is absolute temperature, β gives the mean free energy, E , of sorption per molecule of sorbate, K_R (L g⁻¹) and a_R (L mg⁻¹) are the R–P constants, α is an exponent, and lies between 0 and 1, K_S is the Sips constant (L mg⁻¹) and $1/n$ is the Sips model exponent.

Table 2
Linear regression coefficients and errors for different isotherm models

Adsorbent	Error	Langmuir	Freundlich	Temkin	D–R	R–P	Sips
KS	R ²	0.9895	0.9398	0.9447	0.7041	0.8064	0.9897
	ARE	9.79	24.95	114.38	245.01	19.83	10.34
	SSE	0.02	0.28	0.05	0.76	0.26	0.01
	HYBRID	0.38	3.38	13.64	49.84	3.15	0.26
	EABS	0.32	1.37	0.74	3.56	1.3	0.28
	MPSD	15.99	32.17	340.15	371.5	27.52	16.63
	χ ²	0.07	0.57	2.32	8.47	0.5	0.04
NaOH–KS	R ²	0.9817	0.8831	0.9517	0.9401	0.4903	0.9962
	ARE	22.68	41.31	128.06	238.13	98.76	7.04
	SSE	0.13	4.92	0.13	1.58	5.07	0.01
	HYBRID	1.46	28.97	17.46	83.02	42.95	0.2
	EABS	1.08	4.02	1.36	4.8	6.96	0.27
	MPSD	33.31	67.14	346.19	332.31	107.62	11.14
	χ ²	0.25	4.92	2.97	14.11	6.87	0.03

concentrations, it reduces to the Langmuir isotherm, which predicts a monolayer adsorption.

The data in Table 3 clearly showed that the adsorption capacity of KS, with a maximum adsorption capacity (q_{max}) of $274.96 \pm 1.55 \text{ mg g}^{-1}$, is much better than other *Artocarpus* fruit wastes such as breadfruit skin [46] and tarap skin [47], magnetite-pectin nanoparticles [48] as well as various adsorbents [50,51]. NaOH treatment significantly enhances the KS's adsorption capacity, to $478.49 \pm 1.15 \text{ mg g}^{-1}$. This is a major finding of this research, and demonstrates the importance of NaOH treatment for CV adsorption.

3.6. Evaluation of thermodynamic parameters

Thermodynamic studies provide information on the feasibility of a chemical process through various parameters, including the standard Gibbs free energy change (ΔG°), standard enthalpy change (ΔH°), and standard entropy change (ΔS°). The Gibbs free energy can be calculated using Eq. (3):

$$\Delta G^\circ = -RT \ln K_c \quad (3)$$

where ΔG° is the Gibbs free energy (kJ mol^{-1}), R is the universal gas constant ($8.314 \text{ J mol}^{-1} \text{ K}^{-1}$), T is the absolute temperature (K), and K_c is the equilibrium constant (C_s/C_e), where C_s is the concentration of dye on the adsorbent (mg L^{-1}) and C_e is the equilibrium dye concentration (mg L^{-1}). The values of ΔH° and ΔS° can be obtained from the plot of the linearized Van't Hoff equation, shown in Eq. (4).

$$\ln K_c = -\frac{\Delta H^\circ}{RT} + \frac{\Delta S^\circ}{R} \quad (4)$$

Thermodynamic studies of CV adsorption onto both KS and NaOH-KS performed within the temperature range 298–344 K indicated that the adsorption was endothermic

Table 3
Adsorption q_{max} values for CV and adsorbents reported in the literature (based on the best experimental conditions in each case)

Adsorbent	q_{max} (mg g^{-1})	Reference
KS	275	This work
NaOH–KS	479	This work
Peat	108	[20]
<i>Cucumis sativus</i> seeds	33	[40]
H ₂ SO ₄ -activated <i>Cucumis sativus</i> seeds	35	[40]
Date palm fiber	269	[41]
Spent tea leaves	115	[42]
Water hyacinth modified with sodium dodecyl sulfate surfactant	116	[43]
Waste apricot activated carbon	58	[44]
Male coconut flowers	60	[22]
Phosphoric acid activated Sulfuric acid activated	86	
Coniferous <i>Pinus</i> bark powder	33	[45]
<i>Artocarpus altilis</i> (Breadfruit) skin	146	[46]
<i>Artocarpus odoratissimus</i> (Tarap) skin	118	[47]
NaOH-treated <i>A. odoratissimus</i> (Tarap) skin	195	[47]
Magnetite/silica/pectin nanoparticles	180	[48]
Magnetite/pectin nanoparticles	72	[48]
Yeast-treated peat	18	[49]

Table 4
Thermodynamic parameters for adsorption of 1,000 mg L⁻¹ CV by KS and NaOH-KS

Temperature (K)	KS			NaOH-KS		
	ΔG° (kJ mol ⁻¹)	ΔH° (kJ mol ⁻¹)	ΔS° (J mol ⁻¹ K ⁻¹)	ΔG° (kJ mol ⁻¹)	ΔH° (kJ mol ⁻¹)	ΔS° (J mol ⁻¹ K ⁻¹)
298	0.63			-3.41		
314	-0.47			-4.94		
324	-0.63	18.31	59.33	-5.62	15.26	63.41
334	-1.65			-5.52		
344	-1.16			-4.99		

and spontaneous, as indicated by the positive ΔH° and negative ΔG° values (Table 4). These results are similar to those reported for treated ginger waste [29], wood apple shells [52], and mango seed kernels [53]. The ΔG° values for NaOH-KS are more negative than those for KS, further supporting enhancement of adsorption by NaOH treatment. The ΔG° values for KS and NaOH-KS both decreased with decreasing temperature from 298 to 344 K, indicating that CV adsorption is more favorable at higher temperatures.

The ΔS° values in Table 4 indicated that both adsorbents showed increasing randomness at the adsorbent-dye solution interface during adsorption. However, the higher ΔS° observed for NaOH-KS could be caused by structural changes arising from interactions of CV and the functional groups of NaOH-KS [54].

3.7. Kinetics studies of CV adsorption

Of the kinetics models commonly used in adsorption studies, three models, i.e., the Lagergren pseudo-first-order [55], Ho's pseudo-second-order [56], and Webber-Morris intraparticle diffusion [57] models were chosen for this study. The linear form of the Lagergren pseudo-first-order kinetic model is expressed as follows:

$$\ln(q_e - q_t) = \ln(q_e) - \frac{k_1}{2.303} t \quad (5)$$

where q_t and q_e (mg g⁻¹) are the adsorption capacities at time t (min) and equilibrium, respectively, and k_1 is the rate constant for pseudo-first-order adsorption (min⁻¹). The values of q_e and k_1 can be determined from the intercept and slope, respectively, of the plot of $\ln(q_e - q_t)$ vs. t .

The linear form of the Ho's pseudo-second-order model is expressed by Eq. (6):

$$\frac{t}{q_t} = \frac{q_e}{k_2 q_e^2} + \frac{1}{q_e} t \quad (6)$$

where k_2 (g mg⁻¹ min⁻¹) is the rate constant.

The initial adsorption rate, h (mg g⁻¹ min⁻¹), is calculated from the pseudo-second-order kinetic parameters using Eq. (7):

$$h = k_2 q_e^2 \quad (7)$$

The kinetics of CV adsorption onto KS and NaOH-KS were investigated using 1,000 mg L⁻¹ CV solution. A high concentration of the adsorbate is necessary for such studies because pseudo kinetics models require a large excess of the reactant. Linear plots of the kinetics models are shown in Fig. 7(a) and (b) and the parameters determined together with the error values are given in Table 5. Although the pseudo-first-order model gave good linear regressions, i.e., 0.9788 and 0.9751 for KS and NaOH-KS, respectively, the $q_{e,calc}$ values were not in close agreement with the experimental values of 236.62 and 432.46 mg g⁻¹ obtained using 1,000 mg L⁻¹ CV. The $q_{e,calc}$ values obtained for KS and NaOH-KS using the pseudo-second-order model are closer to the experimental values. These results were further confirmed by fitting the kinetics parameters to the error functions, i.e., ARE, SSE, HYBRID, and χ^2 , to obtain the lowest error values, listed in Table 5; lower error values are observed for the pseudo-second-order model.

The intraparticle diffusion model [64], which is used to predict transport of an adsorbate from the exterior surface to the pores of the adsorbent, provides information regarding the steps involved in the adsorption process. The basic equation for intraparticle diffusion is given by Eq. (8).

$$q_t = k_{id} t^{1/2} + C \quad (8)$$

where k_{id} (mg g⁻¹ min^{-0.5}) represents the intraparticle diffusion rate constant and C (mg g⁻¹) is the thickness of the boundary layer.

Although the linear plots of the intraparticle diffusion model in Fig. 7(c) give good R^2 values for both KS (0.9598) and NaOH-KS (0.9369), they do not pass through the origin, implying that this diffusion model is not the rate-limiting step in the adsorption process.

The Boyd kinetic model [58], a valuable tool in understanding the actual rate-limiting step of an adsorbate-adsorbent system, is given by Eq. (9)

$$F = 1 - \frac{6}{R^2} \exp(-B_t) \quad (9)$$

and Eq. (10)

$$F = \frac{q_t}{q_e} \quad (10)$$

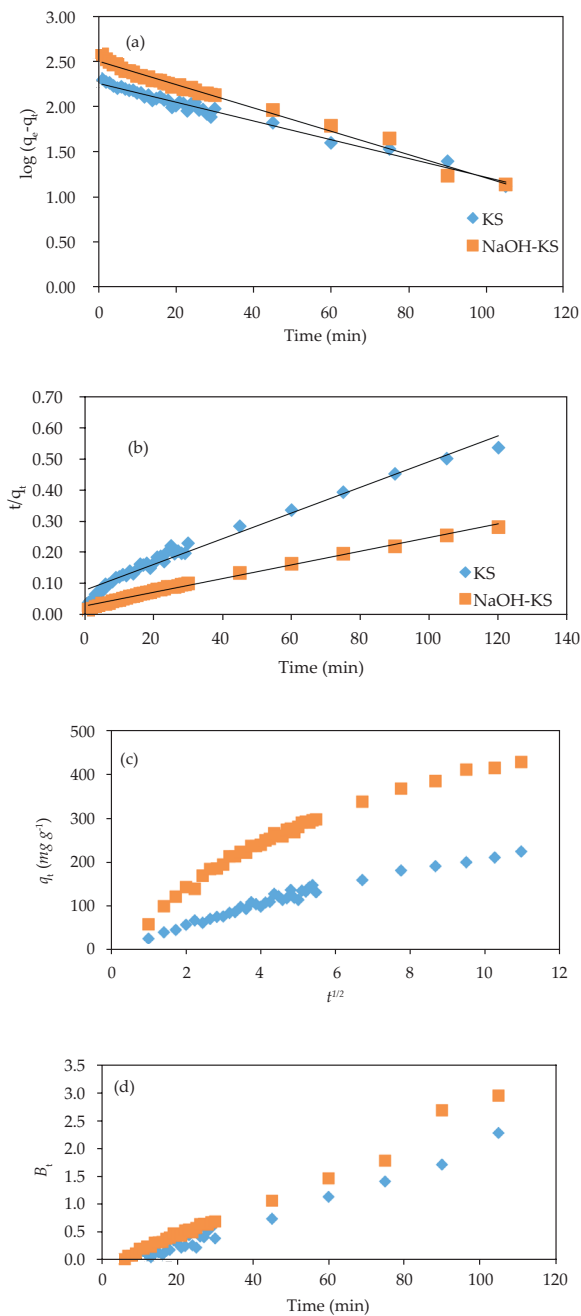


Fig. 7. Pseudo-first-order (a), pseudo-second-order (b), Intraparticle diffusion (c) and Boyd plots (d) kinetic plots for adsorption of CV (initial concentration 1000 mg L^{-1}) on KS and NaOH-KS.

where F is the fraction of solute adsorbed at time t and B_t is a mathematical function of F .

Rearranging Eq. (10) gives the following:

$$B_t = -0.4977 - \ln(1-F) \quad (11)$$

The Boyd's plot of B_t vs. t can be used to distinguish between film diffusion (external transport) and intraparticle diffusion. If the linear plot passes through the origin, the adsorption process is predicted to follow an intraparticle

Table 5

Kinetic model parameters for adsorption of $1,000 \text{ mg L}^{-1}$ CV on KS and NaOH-KS

Parameters	KS	NaOH-KS
Pseudo-first-order model		
$q_{e,calc} \text{ (mg g}^{-1}\text{)}$	62.29	311.53
$k_1 \text{ (min}^{-1}\text{)}$	0.02	0.03
R^2	0.9788	0.9851
ARE	45.62	49.22
SSE	0.57	3.35
EABS	4.43	10.79
HYBRID	6.51	17.3
χ^2	2.15	5.71
Pseudo-second-order model		
$q_{e,calc} \text{ (mg g}^{-1}\text{)}$	243.90	454.55
$k_2 \text{ (g mg}^{-1} \text{ min}^{-1}\text{)}$	0.0002	0.0002
$h \text{ (mg g}^{-1} \text{ min}^{-1}\text{)}$	11.90	41.32
R^2	0.9764	0.9905
ARE	11.07	9.77
SSE	0.03	0.14
EABS	0.86	1.68
HYBRID	0.56	1.12
χ^2	0.19	0.37
$q_{e,exp} \text{ (mg g}^{-1}\text{)}$	235.96	432.58
Intraparticle diffusion		
$k_{id} \text{ (mg g}^{-1} \text{ min}^{-0.5}\text{)}$	19.62	35.12
R^2	0.9598	0.9369
Boyd		
$D_i \text{ (}\times 10^{-5} \text{ cm}^2 \text{ s}^{-1}\text{)}$	5.5	9.7
R^2	0.9369	0.9807

diffusion mechanism; otherwise, the adsorption process is controlled by film diffusion or external mass transport. Film diffusion occurs when the adsorbate ions travel toward the external surface of the adsorbent, whereas in particle diffusion, the adsorbate ions travel within the pores of the adsorbent. The Boyd's plot in Fig. 7(d) did not pass through the origin, for both KS and NaOH-KS, indicating that the adsorption processes were mainly controlled by external mass transport or film diffusion.

The calculated B_t values are used to calculate the effective diffusion coefficient $D_i \text{ (cm}^2 \text{ s}^{-1}\text{)}$ using Eq. (12).

$$D_i = \frac{B_t r^2}{\pi^2} \quad (12)$$

where $r \text{ (cm)}$ is the radius of the adsorbent calculated by sieve analysis; the D_i values calculated assuming spherical particles of radius 0.0425 cm for KS and NaOH-KS are listed in Table 5. The average D_i values for the adsorption of CV on KS and NaOH-KS are estimated to be 5.50×10^{-5} and $9.70 \times 10^{-5} \text{ cm}^2 \text{ s}^{-1}$, respectively.

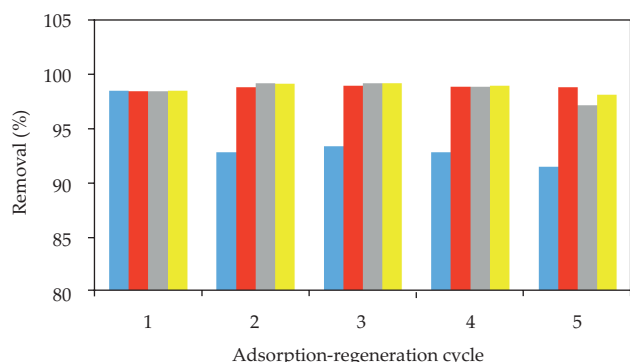


Fig. 8. CV removals by NaOH-KS regenerated using (●) 0.1 M HNO₃, (●) 0.1 M NaOH, (●) water, and (●) control for five consecutive cycles.

3.8. Regeneration of NaOH-KS

KS and NaOH-KS both showed good CV-adsorption capacities. It is beneficial if adsorbents can be regenerated and reused for a number of cycles. This reduces the amounts of treated adsorbent for disposal [59]. NaOH-KS, which has a better CV-adsorption capacity than KS, was used to investigate the possibility of reusing the adsorbent in at least five consecutive cycles, to determine the feasibility and practicality of its use in real wastewater treatments. NaOH-KS was first loaded with 100 mg L⁻¹ CV and the dye-loaded NaOH-KS was washed with either 0.1 M HNO₃, 0.1 M NaOH, or water. A control (without washing) was kept for comparison. The removal efficiencies of the regenerated NaOH-KS samples are shown in Fig. 8.

The CV-removal efficiency of NaOH-KS regenerated with acid decreased from 98% to 91% from cycles 1 to 5. Similar results were obtained for regeneration with water and the control. For water regeneration, more than 90% removal was achieved in cycle 1 and the ability to remove the dye decreased to 97% in cycle 5. Of the methods used, regeneration with 0.1 M NaOH was the best, and the adsorbent was still able to remove CV after the fifth cycle, maintaining an excellent removal efficiency of 99%. NaOH-KS therefore has great potential for use in real wastewater treatments because it can be regenerated and able to maintain a high adsorptive capacity for several cycles. This is an advantage in terms of cost management.

4. Conclusion

A. camansi peel is a low-cost and effective biosorbent for the removal of CV from aqueous solutions. We conclusively showed that chemical modification of *A. camansi* peel by treatment with 4.0 M NaOH, to give NaOH-KS, improves the adsorption capacity (q_{max}) by more than 70%, and shortens the time taken for adsorption to reach equilibrium. Chemical treatment with NaOH probably deprotonates acidic functionalities of KS, such as phenolic and carboxylic acid groups, making them anionic; they therefore attract positively charged CV molecules. Treatment of NaOH-KS with CV decreases the metal ion content of the

adsorbent, in particular those of Na, Mg, and Ca, implying that ion exchange plays a role when CV is attracted to NaOH-KS. Additional evidence for the stronger affinity of NaOH-KS for CV was provided by experimental determination of thermodynamic parameters. The average standard Gibbs free energy of attraction for CV and NaOH-KS in the temperature range 298 to 344 K is much more negative than the corresponding value for natural KS. After CV adsorption, the NaOH-KS adsorbent can be effectively regenerated, without losing its effectiveness, by treatment with NaOH.

Acknowledgements

The authors would like to thank the Government of Negara Brunei Darussalam and the Universiti Brunei Darussalam (UBD) for their financial support. The authors are also grateful to the Centre of Advanced Material and Energy Science (CAMES) and Department of Biology for the use of XRF, SEM and temperature-controlled water bath shaker.

References

- [1] H. Gao, T. Kan, S. Zhao, Y. Qian, X. Cheng, W. Wu, X. Wang, L. Zheng, Removal of anionic azo dyes from aqueous solution by functional ionic liquid cross-linked polymer, *J. Hazard. Mater.*, 261 (2013) 83–90.
- [2] N. Priyantha, L.B.L. Lim, S. Wickramasooriya, Adsorption Behavior of Cr(VI) by Muthurajawela Peat, *Desalin. Water Treat.*, 57 (2016) 16592–16600.
- [3] M.R.R. Kooh, M.K. Dahri, L.B.L. Lim, The use of a lignocellulosic material, *Casuarina equisetifolia* needle, as a sustainable adsorbent for the removal of hazardous Rhodamine B dye from water, *Cogent Environ. Sci.*, (2016) doi: 10.1080/23311843.2016.1140553
- [4] M.R.R. Kooh, M.K. Dahri, L.B.L. Lim, L.H. Lim, Batch adsorption studies on the removal of acid blue 25 from aqueous solution using *Azolla pinnata* and soya bean waste, *Arab. J. Sci. Eng.*, (2015) doi: 10.1007/s13369-015-1877-5
- [5] M.T. Amin, A.A. Alazba, M. Shafiq, Adsorption of copper (Cu²⁺) from aqueous solution using date palm trunk fibre: isotherms and kinetics, *Desalin. Water Treat.*, (2015) doi:10.1080/19443994.2015.1131635
- [6] A. Bhatnagar, M. Sillanpää, A. Witek-Krowiak, Agricultural waste peels as versatile biomass for water purification—A review, *Chem. Eng. J.*, 270 (2015) 244–271.
- [7] L.B.L. Lim, N. Priyantha, D.T.B. Tennakoon, T. Zehra, Sorption characteristics of peat of Brunei Darussalam. II: interaction of aqueous copper(II) species with raw and processed peat, *J. Ecol. Technol. Res.*, 17 (2013) 45–49.
- [8] L.B.L. Lim, N. Priyantha, D.T.B. Tennakoon, H.I. Chieng, C. Bandara, Sorption characteristics of peat of Brunei Darussalam I: characterization of peat and adsorption equilibrium studies of Methylene blue—Peat interactions, *Cey. J. Sci. (Phys. Sci.)*, 17 (2013) 41–51.
- [9] T. Zehra, L.B.L. Lim, N. Priyantha, Removal behavior of peat collected from Brunei Darussalam for Pb(II) ions from aqueous solution: equilibrium isotherm, thermodynamics, kinetics, and regeneration studies, *Environ. Earth. Sci.*, 74 (2015) 2541–2551.
- [10] T. Zehra, N. Priyantha, L.B.L. Lim, E. Iqbal, Sorption characteristics of peat of Brunei Darussalam V: removal of Congo red dye from aqueous solution by peat, *Desalin. Water Treat.*, 54 (2015) 2592–2600.
- [11] L.B.L. Lim, N. Priyantha, U.K. Ramli, H.I. Chieng, Adsorption of Cd(II) ions using Lamiding, a wild vegetable from Brunei Darussalam, *J. Appl. Phytotechnol. Environ. Sanitation*, 3 (2014) 65–74.

- [12] L.B.L. Lim, N. Priyantha, C.M. Chan, D. Matassan, H.I. Chieng, M.R.R. Kooh, Investigation of the sorption characteristics of water lettuce (WL) as a potential low-cost biosorbent for the removal of methyl violet 2B, *Desalin. Water Treat.*, 57 (2016) 8319–8329.
- [13] M.K. Dahri, H.I. Chieng, L.B.L. Lim, N. Priyantha, C.C. Mei, Cempedak Durian (*Artocarpus* sp.) peel as a biosorbent for the removal of toxic methyl violet 2B from aqueous solution, *Korean Chem. Eng. Res.*, 53 (2015) 576–583.
- [14] L.B.L. Lim, N. Priyantha, D.T.B. Tennakoon, H.I. Chieng, M.K. Dahri, M. Suklueng, Breadnut peel as a highly effective low-cost biosorbent for methylene blue: equilibrium, thermodynamic and kinetic studies, *Arab. J. Chem.*, (2013) <http://dx.doi.org/10.1016/j.arabjc.2013.12.018>
- [15] F.A. Pavan, E.S. Camacho, E.C. Lima, G.L. Dotto, V.T.A. Branco, S.L.P. Dias, Formosa papaya seed powder (FPSP): preparation, characterization and application as an alternative adsorbent for the removal of crystal violet from aqueous phase, *J. Environ. Chem. Eng.*, 2 (2014) 230–238.
- [16] M.K. Dahri, M.R.R. Kooh, L.B.L. Lim, Water remediation using low cost adsorbent walnut shell for removal of malachite green: equilibrium, kinetics, thermodynamic and regeneration studies, *J. Environ. Chem. Eng.*, 2 (2014) 1434–1444.
- [17] L.B.L. Lim, H.I. Chieng, F.L. Wimmer, Nutrient composition of *Artocarpus champeden* and its hybrid (Nanchem) in Negara Brunei Darussalam, *ASEAN J. Sci. Technol.*, 28 (2011) 122–138.
- [18] Y.P. Tang, B.L.L. Linda, L.W. Franz, Proximate analysis of *Artocarpus odoratissimus* (Tarap) in Brunei Darussalam, *Int. Food. Res. J.*, 20 (2013) 409–415.
- [19] N.A. Littlefield, B.N. Blackwell, C.C. Hewitt, D.W. Gaylor, Chronic toxicity and carcinogenicity studies of gentian violet in mice, *Fundam. Appl. Toxicol.*, 5 (1985) 902–912.
- [20] H.I. Chieng, L.B.L. Lim, N. Priyantha, D.T.B. Tennakoon, Sorption characteristics of peat of Brunei Darussalam III: equilibrium and kinetics studies on adsorption of crystal violet (CV), *Int. J. Earth. Sci. Eng.*, 6 (2013) 791–801.
- [21] S. Senthilkumaar, P. Kalaamani, C.V. Subburaam, Liquid phase adsorption of crystal violet onto activated carbons derived from male flowers of coconut tree, *J. Hazard. Mater.*, 136 (2006) 800–808.
- [22] L.B.L. Lim, N. Priyantha, H.I. Chieng, M.K. Dahri, *Artocarpus camansi* Blanco (Breadnut) core as low-cost adsorbent for the removal of methylene blue: equilibrium, thermodynamics and kinetics studies, *Desalin. Water Treat.*, 57 (2016) 5673–5685.
- [23] N. Priyantha, L.B.L. Lim, D.T.B. Tennakoon, N.H. Mohd Mansor, M.K. Dahri, H.I. Chieng, Breadfruit (*Artocarpus altilis*) waste for bioremediation of Cu(II) and Cd(II) ions from aqueous medium, *Ceyl. J. Sci.*, 17 (2013) 19–29.
- [24] L.B.L. Lim, N. Priyantha, D.T.B. Tennakoon, M.K. Dahri, Biosorption of cadmium(II) and copper(II) ions from aqueous solution by core of *Artocarpus odoratissimus*, *Environ. Sci. Pollut. Res.*, 19 (2012) 3250–3256.
- [25] L.B.L. Lim, N. Priyantha, M.H.F. Lai, R.M. Salleha, T. Zehra, Utilization of *Artocarpus* hybrid (Nanchem) skin for the removal of Pb(II): equilibrium, thermodynamics, kinetics and regeneration studies, *Int. Food. Res. J.*, 22 (2015) 1043–1052.
- [26] M.K. Dahri, L.B.L. Lim, C.C. Mei, Cempedak durian as a potential biosorbent for the removal of Brilliant Green dye from aqueous solution: equilibrium, thermodynamics and kinetics studies, *Environ. Monitor. Assess.*, 187 (2015) 546, doi: 10.1007/s10661-015-4768-z
- [27] M.K. Dahri, L.B.L. Lim, N. Priyantha, C.M. Chan, Removal of acid blue 25 using Cempedak Durian peel from aqueous medium: Isotherm, kinetics and thermodynamics studies, *Int. Food Res. J.*, 23 (2016) 1154–1163.
- [28] M.H. Baek, C.O. Ijagbemi, O. Se-Jin, D.S. Kim, Removal of malachite green from aqueous solution using degreased coffee bean, *J. Hazard. Mater.*, 176 (2010) 820–828.
- [29] R. Kumar, R. Ahmad, Biosorption of hazardous crystal violet dye from aqueous solution onto treated ginger waste (TGW), *Desalin.*, 265 (2011) 112–118.
- [30] L.B.L. Lim, N. Priyantha, D.T.B. Tennakoon, M.K. Dahri, H. I. Chieng, T. Zehra, M. Suklueng, *Artocarpus odoratissimus* skin as potential low-cost biosorbent for the removal of methylene blue and methyl violet 2B, *Desalin. Water Treat.*, 53 (2015) 964–975.
- [31] H.I. Chieng, L.B.L. Lim, N. Priyantha, Sorption characteristics of peat from Brunei Darussalam for the removal of rhodamine B dye from aqueous solution: adsorption isotherms, thermodynamics, kinetics and regeneration studies, *Desalin. Water Treat.*, 55 (2015) 664–677.
- [32] L.B.L. Lim, N. Priyantha, C.M. Chan, D. Matassan, H.I. Chieng, M.R.R. Kooh, Adsorption behavior of methyl violet 2B using Duckweed: equilibrium and kinetics studies, *Arab. J. Sci. Eng.*, 39 (2014) 6757–6765.
- [33] H.I. Chieng, T. Zehra, L.L. Lim, N. Priyantha, D.T.B. Tennakoon, Sorption characteristics of peat of Brunei Darussalam IV: equilibrium, thermodynamics and kinetics of adsorption of methylene blue and malachite green dyes from aqueous solution, *Environ. Earth. Sci.*, 72 (2014) 2263–2277.
- [34] H. Tang, W. Zhou, L. Zhang, Adsorption isotherms and kinetics studies of malachite green on chitin hydrogels, *J. Hazard. Mater.*, 209–210 (2012) 218–225.
- [35] M.M. Dubinin, L.V. Radushkevich, Equation of the characteristic curve of activated charcoal, *Proc. Acad. Sci.*, 55 (1947) 327.
- [36] M.J. Temkin, V. Pyzhev, Kinetics of ammonia synthesis on promoted iron catalysts, *Acta. Physiochim.*, 12 (1940) 217.
- [37] H. Freundlich, Over the adsorption in the solution, *J. Phys. Chem.*, 57 (1906) 385–470.
- [38] I. Langmuir, The adsorption of gases on plane surfaces of glass, mica and platinum, *J. Am. Chem. Soc.*, 40 (1918) 1361–1403.
- [39] R. Sips, Combined form of Langmuir and Freundlich equations, *J. Chem. Phys.*, 16 (1948) 490–495.
- [40] T. Smitha, T. Santhi, A.L. Prasad, S. Manonmani, *Cucumis sativus* used as adsorbent for the removal of dyes from aqueous solution, *Arab. J. Chem.*, (2012) doi: 10.1016/j.arabjc.2012.1007.1030.
- [41] M. Alshabanat, G. Alsenani, R. Almufarj, Removal of crystal violet dye from aqueous solutions onto date palm fiber by adsorption technique, *J. Chem. Phys.*, (2013) doi: <http://dx.doi.org/10.1155/2013/210239>.
- [42] S.K. Bajpai, A. Jain, Equilibrium and thermodynamic studies for adsorption of crystal violet onto spent tea leaves (STL), *Water. J.*, (2012) doi: 10.14294/WATER.12012.14295.
- [43] E. Sanmuga Priya, P. Senthamil Selvan, Water hyacinth (*Eichhornia crassipes*)—An efficient and economic adsorbent for textile effluent treatment—A review, *Arab. J. Chem.*, (2014) doi: 10.1016/j.arabjc.2014.1003.1002.
- [44] C.A. Başar, Applicability of the various adsorption models of three dyes adsorption onto activated carbon prepared waste apricot, *J. Hazard. Mater.*, 135 (2006) 232–241.
- [45] R. Ahmad, Studies on adsorption of crystal violet dye from aqueous solution onto coniferous pinus bark powder (CPBP), *J. Hazard. Mater.*, 171 (2009) 767–773.
- [46] L.B.L. Lim, N. Priyantha, N.H. Mohd Mansor, *Artocarpus altilis* (breadfruit) skin as a potential low-cost biosorbent for the removal of crystal violet dye: equilibrium, thermodynamics and kinetics studies, *Environ. Earth Sci.*, 73 (2015), 3239–3247.
- [47] L.B.L. Lim, N. Priyantha, T. Zehra, C.W. Then, C.M. Chan, Adsorption of crystal violet dye from aqueous solution onto *Artocarpus odoratissimus* skin and its NaOH-treated form: equilibrium and kinetics studies, *Desalin. Water Treat.*, 57 (2016) 10246–10260.
- [48] O.A. Attallah, M.A. Al-Ghobashy, M. Nebsen, M.Y. Salem, Removal of cationic and anionic dyes from aqueous solution with magnetite/pectin and magnetite/silica/pectin hybrid nanocomposites: Kinetic, isotherm and mechanism analysis, *RSC Adv.*, 6 (2016) 11461–11480.
- [49] T. Zehra, N. Priyantha, L.B.L. Lim. Removal of crystal violet dye from aqueous solution using yeast-treated peat as adsorbent: Thermodynamics, kinetics, and equilibrium studies. *Environ. Earth Sci.*, 75 (2016) 1–15. doi 10.1007/s12665-016-5255-8
- [50] L.B.L. Lim, N. Priyantha, H.H. Cheng, N.A.H. Mohamad Zaidi. Adsorption characteristics of *Artocarpus odoratissimus* leaf toward removal of toxic Crystal violet dye: isotherm, thermodynamics and regeneration studies, *J. Environ. Biotechnol. Res.*, 4 (2016) 32–40.

- [51] L.B.L. Lim, N. Priyantha, H.H. Cheng, N.A.H. Mohamad Zaidi, Parkiaspeciosa (Petai) pod as a potential low-cost adsorbent for the removal of toxic crystal violet dye, *Scientia Bruneiana Special issue.*, 15 (2016) 99–106.
- [52] S. Jain, R.V. Jayaram, Removal of basic dyes from aqueous solution by low-cost adsorbent: wood apple shell (*Feronia acidissima*), *Desalin.*, 250 (2010) 921–927.
- [53] K.V. Kumar, A. Kumaran, Removal of methylene blue by mango seed kernel powder, *Biochem. Eng. J.*, 27 (2005) 83–93.
- [54] K.G. Bhattacharyya, A. Sharma, Adsorption of Pb(II) from aqueous solution by *Azadirachta indica* (Neem) leaf powder, *J. Hazard. Mater.*, 113 (2004) 97–109.
- [55] S. Lagergren, About the theory of so-called adsorption of soluble substances, *K. Sven. Vet. Akad. Handl.*, 24 (1898) 1–39.
- [56] Y.S. Ho, G. McKay, Sorption of dye from aqueous solution by peat, *Chem. Eng. J.*, 70 (1998) 115–124.
- [57] W.J. Weber, J.C. Morris, Kinetics of adsorption on carbon from solution, *J. Sanitary Eng. Div. Am. Soc. Chem. Eng.*, 89 (1963) 31–59.
- [58] G.E. Boyd, A.W. Adamson, L.S. Myers Jr., The exchange adsorption of ions from aqueous solutions by organic zeolites. II. Kinetics 1, *J. Am. Chem. Soc.*, 69 (1947) 2836–2848.
- [59] H.I. Chieng, L.B.L. Lim, N. Priyantha, Enhancing adsorption capacity of toxic malachite green dye through chemically modified breadnut peel: equilibrium, thermodynamics, kinetics and regeneration studies, *Environ. Technol.*, 36 (2015) 86–97.